

HOW TO CHARACTERIZE YIELD STRESS FLUIDS WITH CAPILLARY BREAKUP EXTENSIONAL RHEOMETRY (CABER)?

K. NIEDZWIEDZ^{*1}, O. ARNOLDS¹, N. WILLENBACHER¹, R. BRUMMER²

¹ Institute of Mechanical Process Engineering and Mechanics, Karlsruhe University,
76131 Karlsruhe, Germany

² Department of Rheology/Thermal Analysis, Beiersdorf AG, 20253 Hamburg, Germany

* Email: katarzyna.niedzwiedz@mvm.uni-karlsruhe.de

Fax: x49.721.6083758

Received: 23.1.2009, Final version: 7.5.2009

ABSTRACT:

Filament breakup of high viscosity fluids with apparent yield stress has been investigated and strategies for an appropriate characterization of their behavior in CaBER experiments are discussed. Filament profiles of such fluids exhibit significant concave curvature. Accurate determination of filament shape is mandatory for understanding deformation behavior. Therefore, we have set up an optical train including high-speed camera, telecentric objective and telecentric back-light illumination with a blue light emitting diode (LED) providing high contrast filament shape imaging. Image analysis allows for diameter determination with an accuracy of $3.55 \mu\text{m}/\text{pixel}$. In addition to the transient filament diameter at the neck we have extracted the curvature at this point as a function of time and the region of deformation, in order to characterize the extensional flow behavior. We have investigated the time evolution of filament shape as a function of various experimental parameters like stretching time, velocity profile during stretching, stretching ratio and initial sample volume at constant stretching ratio. Filament thinning is independent of stretching time, t_s , and stretching velocity profile. But when the same stretching ratio is applied at different initial volume fraction, filament curvature increases strongly with decreasing sample volume leading to an increase of filament life time according to the negative contribution of its curvature to the Laplace pressure inside the fluid.

ZUSAMMENFASSUNG:

Es wurde der Fadenabriss von hochviskosen Flüssigkeiten mit scheinbarer Fließgrenze untersucht und Strategien für die Charakterisierung ihres Verhaltens in CaBER Experimenten diskutiert. Das Fadenprofil solcher Flüssigkeiten zeigt eine signifikante konkave Krümmung. Daher ist die präzise Charakterisierung der Fadenkonturen für das Verstehen des Deformationsverhaltens entscheidend. Aus diesem Grund wurde der optische Aufbau des CaBER Gerätes mit einer Hochgeschwindigkeitskamera, telezentrischen Objektiven und blauer, telezentrischer Hintergrundbeleuchtung, die eine kontrastreiche Fadenkonturabbildung ergibt, ausgestattet. Die Bildanalyse lässt eine hochauflösende Durchmesserbestimmung mit der Genauigkeit von $\pm 3.55 \mu\text{m}/\text{pixel}$ zu. Zusätzlich zum zeitlichen Verlauf des Durchmessers an der Fadeneinschnürung wurden auch der zeitliche Verlauf der Krümmung an dieser Stelle und der Formänderungsbereich berechnet, um das Dehnfließverhalten zu charakterisieren. Die zeitliche Entwicklung der Fadenprofile in Abhängigkeit von unterschiedlichen experimentellen Parametern wie z. B. Dehnzeit t_s , Dehngeschwindigkeitsprofil, Dehnrate und Anfangsprobenvolumen bei konstanter Dehnrate wurde untersucht. Die Fadenverdünnung ist unabhängig von t_s und dem Dehngeschwindigkeitsprofil. Wird die gleiche Dehnrate bei unterschiedlichem Anfangsprobenvolumen verwendet, steigt die Fadenkrümmung mit abnehmendem Probenvolumen stark an. Dies führt zur Erhöhung der Fadenlebensdauer entsprechend dem negativen Beitrag der Krümmung zum Laplace Druck innerhalb der Flüssigkeit.

RÉSUMÉ:

La rhéologie extensionnelle de fluides de viscosité élevée ayant une contrainte seuil a été étudiée dans le but d'obtenir des connaissances déterminantes sur leur comportement lors de ce type d'écoulement. Les expériences ont été effectuées à l'aide du rhéomètre élongationnel CaBER. Le profil des filaments obtenu pour de tels fluides montrent une courbure concave significative et une détermination précise de leurs formes est nécessaire pour comprendre leur comportement lors de la déformation. Pour cela nous avons équipé notre montage optique d'une caméra à haute vitesse, d'un objectif télécentrique et d'un éclairage d'arrière-plan télécentrique de couleur bleue qui permet d'obtenir un contraste élevé de l'image du filament. L'analyse des images au point de courbure du filament permet une détermination du diamètre au cours du temps avec une précision de l'ordre de $3.55 \mu\text{m}/\text{pixel}$. En plus de la détermination du diamètre, nous avons également étudié l'évolution de la forme de la courbure du filament en fonction du temps en variant divers paramètres expérimentaux tels que : la durée de l'élongation, le profile de vitesse durant l'élongation, le taux d'élongation et le volume initiale de

l'échantillon à taux d'élongation constant. La réduction du filament est indépendante de la durée de l'élongation et du profil de vitesse. Par contre pour un même taux d'élongation appliqué à un volume initial de l'échantillon différent, la courbure du filament augmente fortement lorsque le volume diminue conduisant à une augmentation de la durée de vie du fil selon la contribution négative de sa courbure à la pression de Laplace à l'intérieur du fluide.

KEY WORDS: yield stress fluids, extensional rheology, CaBER, image analysis

1 INTRODUCTION

Understanding of elongational deformation processes is of great importance in many industrial applications. Deformation and breakup of liquid threads is crucial in such processes as spraying and atomization. But even in simple every-day actions e.g., filling in or out bottles, blending, or coating, extensional deformation plays an important role.

Capillary breakup was the subject of scientific discussion already in 19th century [1, 2]. Since then many studies emerged aiming at the understanding of this phenomenon and later on give beginning to extensional rheology. There are various configurations of measurement instruments available for testing extensional deformation. Nowadays FiSER (filament stretching extensional rheometer) [3, 4] and CaBER (capillary breakup extensional rheometer) are among the most common devices for measuring extensional flow properties of low viscosity fluids [5]. In FiSER configurations exponential plate separation is imposed in order to produce elongational deformation with constant deformation rate. The time evolution of tensile force acting on fluid filament and the midpoint filament diameter are measured. In CaBER experiments the sample is filled between two coaxial parallel plates creating a fluid connection between them. The plates are rapidly moved apart from each other creating a step strain deformation. The resulting liquid bridge deforms gradually under the action of visco-elastic and capillary forces, contracts and finally breaks. Here, the only measured parameter is the time evolution of midpoint diameter. The advantage of the CaBER technique is that it can be applied to liquids covering a wide range of extensional viscosities, from about $5 \cdot 10^{-3}$ Pa.s up to nearly 10^4 Pa.s. The technique is straightforward, fast and requires only a small amount of probing sample ($V < 0.1$ ml). In addition, for many fluids large Hencky strains up to $\epsilon = 7$ are attainable.

Investigations on extensional viscosity with FiSER and CaBER technique started with dilute polymer solutions. Such solutions form uniform cylindrical filaments in CaBER experiments and their diameter decays exponentially [6 – 8]. Surprisingly, one has to dilute well below c^* to find that the corresponding relaxation time λ_ϵ agrees well with the shear relaxation time λ_γ determined from small amplitude oscillatory shear experiment [9]. FiSER experiments revealed significant strain hardening for solutions containing even low concentration of high molecular weight polymer [4, 10]. Visco-elastic wormlike micelles solutions exhibit flow behavior similar to polymer solutions [11]. However, unlike polymers, wormlike micelles are self-assembled, this means that they can break apart under large elastic stresses resulting in large differences between extensional viscosities deduced from FiSER and CaBER experiments [12]. Recently capillary breakup rheometry is more and more applied to investigate extensional properties of complex fluids [13 – 15]. These experimental studies were supported by theoretical analysis and numerical simulations. Renardy performed one dimensional analysis for the evolution of the fluid jet based on self-similarity solutions for power law fluids [16, 17], Giesekus [18] and Phan-Thien-Tanner (PTT) [19] models. Further investigations developed more detailed analysis of stretching deformation and breakup. Basaran et al. proved validation of one dimensional approaches carrying out the comparison between one and two dimensional models concerning Newtonian and Carreau fluids. They performed calculations for the time evolution of filament profiles including two dimensional analysis of viscosity and velocity field through out the full length of the liquid bridge [20, 21]. Lately, Webster et al. modeled step-strain deformation of CaBER type configurations [22]. Two dimensional analysis of filament profiles under uniaxial deformation was performed with special regard to differences between Oldroyd-B, Giesekus and PTT models.

Previous studies on the elongation breakup of complex fluids point out that, the shape of the fluid filament is not implicitly cylindrical, but seems to be material specific [13, 15]. Only weakly visco-elastic fluids like dilute and semi-dilute polymer solutions undergo uniform cylindrical filament thinning [14, 23, 24]. Even in the case of the Newtonian liquids, although filaments thin over their full length, thinning is inhomogeneous [13, 25]. The filament shape is slightly concave, adjacent to the plates the diameter is thicker than at the axial break point location. For power law and plastic fluids this effect is even more pronounced. As an illustration a comparison of filament profiles commonly observed for various cosmetic products is shown in Figure 1. Thinning often takes place only within a restricted volume of the filament, and is hardly visible beyond this region. For such filament profiles, the filament diameter and the filament life time strongly depend on the height where they are measured. Neither $\dot{\epsilon}(t)$ nor $\epsilon(t)$ is constant through the filament length. In such cases, it is not enough to measure the decay of the mid-point diameter in order to analyze the thinning process.

First experiments on yield stress fluids have shown, that such fluids can form stable bridges with lengths bigger than 2π times the radius of the cylinder [26, 27]. Goldin et al. pointed at the existence of a critical sample radius, R_c at the neck of filament [28]. As long as $R > R_c$ the capillary pressure does not exceed the value of yield stress, i.e. it is not sufficient to generate flow. The filament stays in static equilibrium and does not evolve in time. However, the processes of thinning and breakup occurring for that kind of liquids are not yet well understood.

We have chosen a highly concentrated w/o emulsion and a semi-dilute acrylic thickener solution as model systems for yield stress fluids. The challenge of this work was to prove the application range of the CaBER technique, to investigate the influence of the experimental parameters on filament thinning of complex fluids with yield stress and to provide suggestions for a meaningful characterization of these fluids with CaBER. Similar studies were performed previously by Rothstein et al. for surfactant and polyelectrolyte solutions as well as polymer blends revealing a strong effect of step-strain parameters on CaBER measurements [29]. They observed

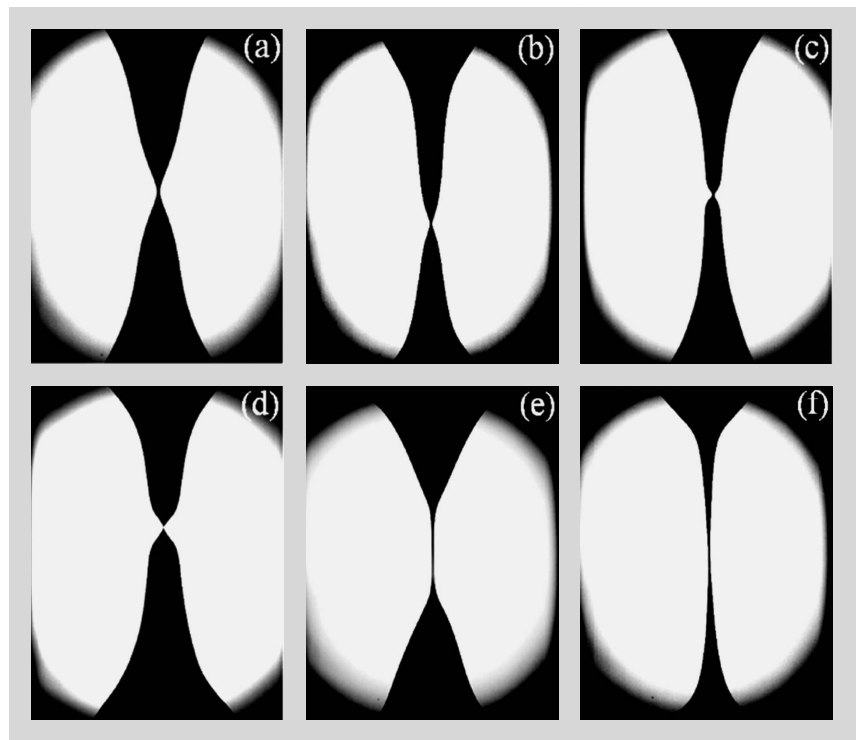


Figure 1: Comparison of filament profiles for different cosmetic products: a) w/o emulsion, b) w/o emulsion, c) w/o creme, d) o/w creme, e) shower gel and f) shampoo.

strong dependence of the imposed extension rates $\dot{\epsilon} = \ln(h_f/h_0)/t_s$ on capillary thinning and filament breakup. In contrast, our experiments show that filament thinning of yield stress fluids is almost independent of imposed stretching time t_s or of stretching velocity profile, but it strongly depends on the initial sample volume, even if the same stretching ratio (Hencky strain) is applied and this is related to the changes in filament curvature. In Section 2 the high resolution optical set-up used to characterize the time evolution of the full filament shape is described. Section 3 concerns the influence of CaBER set-up parameters on filament thinning. Finally, in Section 4 concluding remarks and further perspectives are summarized.

2 EXPERIMENTAL

2.1 SAMPLES

Two distinct products have been used as model systems, a water in oil (w/o) emulsion and a high viscosity thickener solution. Droplet size distribution of the emulsion was determined by static light scattering in the Fraunhofer diffraction limit. Particle size distribution is narrow, the mean particle diameter is $d(0.5) = 0.911 \mu\text{m}$, the values at 10 and 90 % are $d(0.1) = 0.592 \mu\text{m}$ and $d(0.9) = 1.378 \mu\text{m}$, respectively. The phase volume, water:oil is 75:25. This means the emulsion is composed of a quasi-network of densely packed small water droplets in continuous oil phase. The latter essentially consists of a paraffin oil with viscosity of $\eta_s = 22 \text{ mPa}\cdot\text{s}$ (at room temperature $T = 20^\circ\text{C}$). The surface tension of the emulsion was measured to be $\sigma = 52 \text{ mN/m}$.

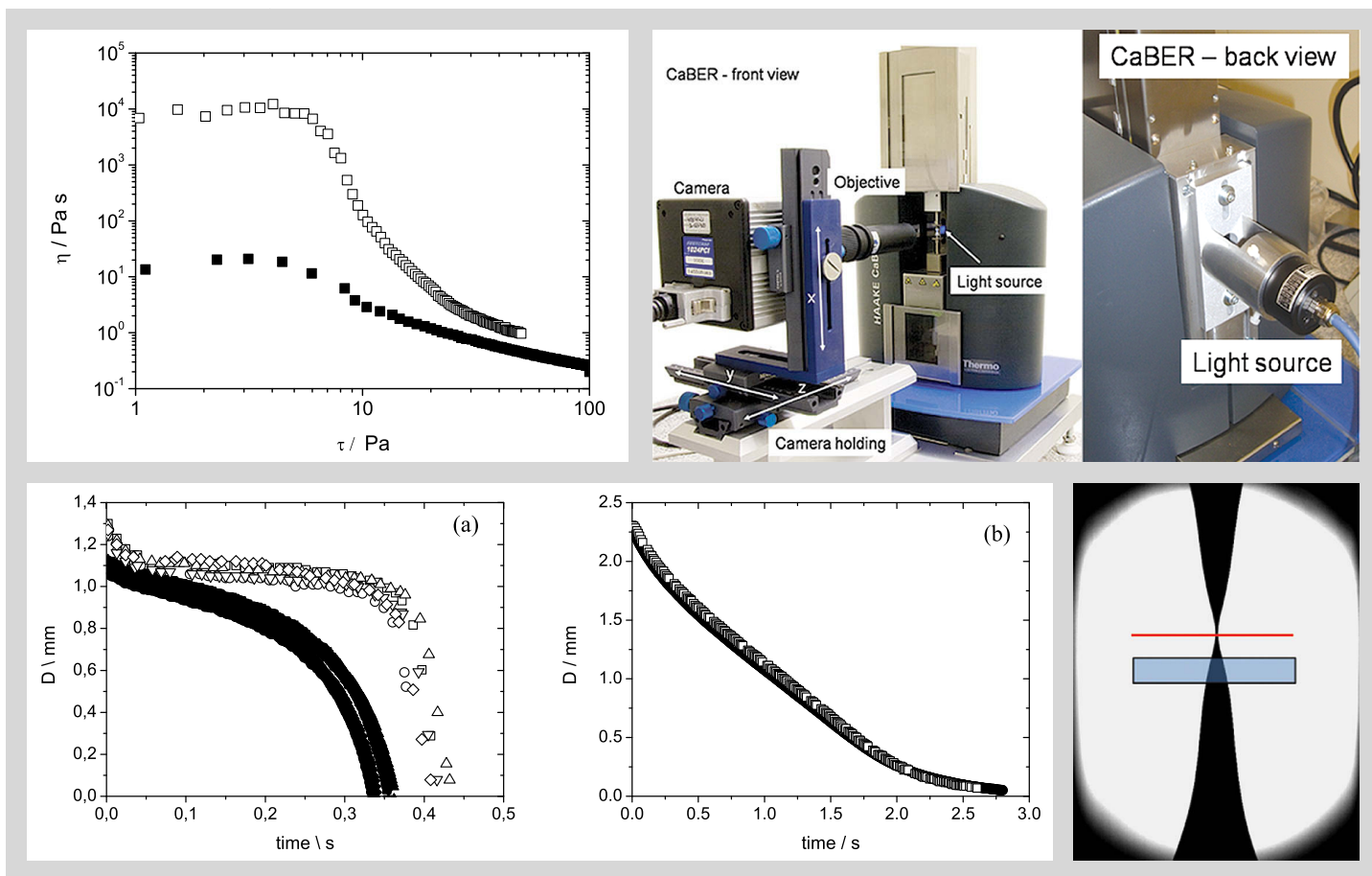


Figure 2 (left above): Steady shear viscosity versus shear stress. Open symbols represent the w/o emulsion and filled symbols correspond to the thickener solution.

Figure 3 (right above): CaBER set-up for image analysis.

Figure 4 (left below): Time evolution of filament diameter obtained from laser measurements (open symbols) and image analysis (filled symbols). Linear stretching profile with stretching time, $t_s = 40$ ms was used. The initial plate distance was $h_0 = 3$ mm, and end plate distance $h_f = 16.64$ mm for the emulsion (a) and $h_f = 10.31$ mm for the poly(ethylene oxide) solution (b).

Figure 5 (right below): Comparison of measurement position provided by laser and image analysis. The line represents spatial resolution gained from image analysis ($16.13 \mu\text{m}$ for 1.06 magnification objective). Height of filament can be freely adjusted to the filament break point. The shaded area corresponds to the 1 mm thick laser beam always probing the average filament diameter around the midpoint.

The thickener solution is based on Sterocoll®D (BASF SE, Ludwigshafen, Germany), which is an alkali swellable polymeric thickener for paper coating. Sterocoll®D is composed of a copolymer of ethylacrylate and (meth)-acrylic acid with molar ratio of acrylate to acid of about 1:1. It is made by emulsion polymerization and is supplied as milky, aqueous dispersion with a solids content of 25 % and a pH of 2.2 - 2.6. The aqueous solution of concentration 2 wt. % was prepared by dilution with deionized water. The pH value was adjusted to pH = 8.4 by slowly adding 1 N NaOH. The solution was stirred at room temperature for 24 h. Due to the covalent crosslinks present in this polymer the dilute neutralized solution resembles the features of a dispersion of highly swollen microgel particles [15].

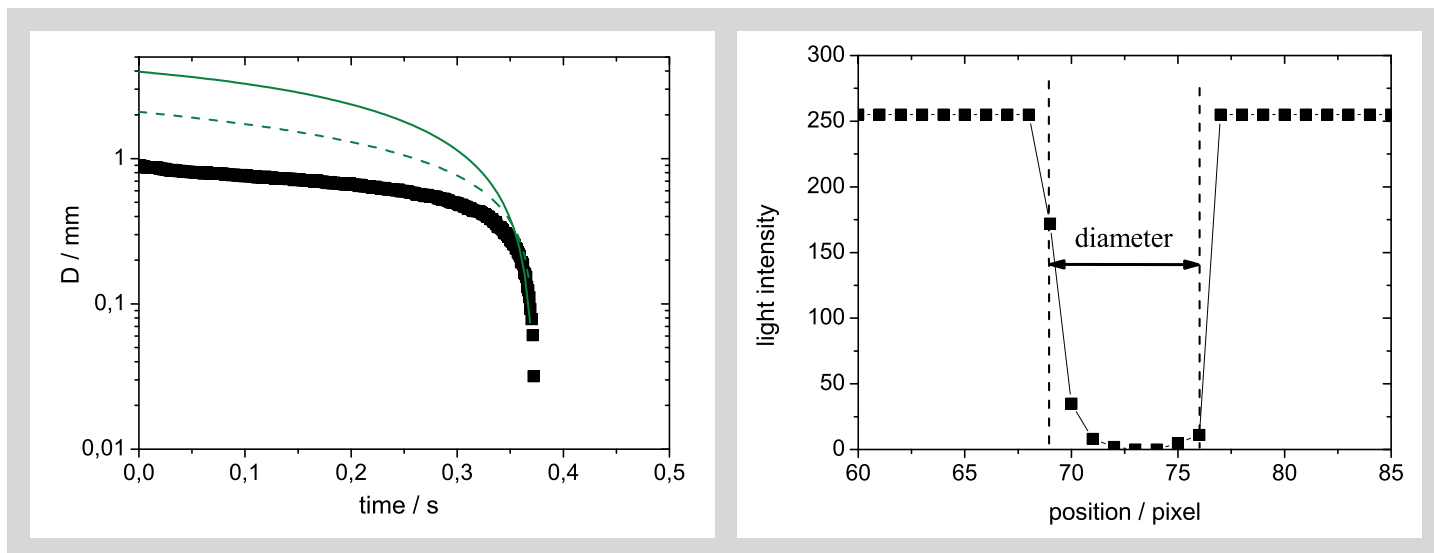
Both samples exhibit plastic flow behavior with power law dependence in steady shear, $\tau = \tau_y + K\dot{\gamma}^n$ with an apparent yield point $\tau_y \approx 10$ Pa. However, the low shear viscosity exhibited by the emulsion is three orders of magnitude higher than the shear viscosity of thickener solution (see Figure 2).

2.2 CABER SET-UP

The commercial CaBER 1 device (Thermo Haake GmbH, Germany), where only the midpoint diameter is measured with a laser micrometer, has been combined with an optical set-up allowing for assess-

ment of full filament shape. The CaBER device with the optical train is shown in Figure 3. The high speed camera, Fastcam-X 1024 PCI (Photron USA, Inc.) is placed in front. It allows to take up to 1000 pictures per second with 1024×1024 pixel resolution. The camera is equipped with telecentric objectives. There are two objectives available, one with 1.06 magnification and one with 5.00 magnification. This corresponds to pixel size of $16.13 \mu\text{m}$ and $3.55 \mu\text{m}$, respectively. Further improvement in resolution is possible using objectives with higher magnification [30] at the expense of the length of the filament that is captured. To improve contrast, the fluid filament is illuminated with a telecentric monochromatic blue light. The illumination source is mounted on the back side of the CaBER device. Illumination takes place via a long hole through the clamp maintaining the plates between which the fluid is placed. To ensure parallel alignment required for telecentric configuration, the camera is mounted on a holder, which can be moved in three dimensions independently changing camera position in x , y and z directions (see Figure 3).

It is worthwhile to note the importance of the telecentric setup for image processing [31]. In conventional imaging systems with entocentric objectives and diffuse illumination image defects appear, which can not be neglected for a detailed quantitative analysis. The common ones are monochromatic aberrations, curvature of the field of image or image distortion and chromatic



ic aberration. In telecentric systems only the light that is parallel to the optical axis passes through and is analyzed. Size and shape of an image formed by such a lens do not depend on the objects distance from the lens and position in the view field. In this way most of the image defects are eliminated. As long as the object stays within the telecentric field always the same size, the real dimension of the object, is pictured. Our new CaBER set-up provides the possibility of simultaneous measurement with laser micrometer and video imaging.

2.3 FILAMENT SHAPE ANALYSIS

Comparison of the results obtained for w/o emulsion from laser micrometer and image analysis is shown in Figure 4a. It can be seen that, though the reproducibility in both cases is comparable, the filament diameters show different thinning behavior. Filament diameter measured by laser is thicker and the filament life time is longer compared with the results obtained from image analysis. This is different from the case of cylindrical filaments where both methods are in perfect agreement (see Figure 4b). A 2 wt. % solution of poly(ethylene oxide) ($M_w = 2 \cdot 10^6$ g/mol) in water was used as a weakly elastic reference fluid forming uniform cylindrical filaments. In case of non-cylindrical filaments the thinning place is not fixed to the filament midpoint, so that the neck is not necessarily at the height of the laser beam. Furthermore, the laser beam averages over a height of 1 mm along the filament axis, compared to $16.13 \mu\text{m}$ camera resolution (for the 1.06 magnification objective), as schematically shown in Figure 5. For that reason, the laser measurements lead to systematic deviations and are inappropriate to investigate non-cylindrical profiles formed e.g. by emulsions with yield stresses or highly visco-elastic polymer solutions [15].

Furthermore, it should be pointed out, that the analysis of the filament diameter at the neck is not

sufficient to extract rheological parameters even with reasonable constitutive equations. Figure 6 compares experimental results for the transient diameter at the neck point measured for the w/o emulsion with theoretical predictions for power-law and Bingham fluids based on a simplified analysis assuming uniform deformation of cylindrical filaments [13]. The dashed line shows the prediction for the power law model:

$$D(t) = \phi(n) D_o \frac{\sigma}{K} (t - t_c)^n \quad (1)$$

where $\phi(n) = 0.0709 + 0.2388(1 - n) - 0.5479(1 - n)^2 + 0.2848(1 - n)^3$, $D_o = 0.9$ mm, filament life time, $t_c = 0.37$ s and the power law parameters extracted from the shear experiment, $K = 3.23$ and $n = 0.62$. The solid line represents the Bingham model:

$$D(t) = \frac{2\sigma}{\tau_y \sqrt{3}} \left(1 - \exp\left(\tau_y \frac{(t - t_c)}{2\sqrt{3}\mu} \right) \right) \quad (2)$$

The calculation was done using the following parameters extracted from shear experiments $\tau_y = 10$ Pa and for μ the limiting plateau viscosity reached at high shear rates was taken, $\mu = 1$ Pa·s. Obviously, the models investigated here can not describe the time evolution of the neck diameter for this fluid. This failure is supposed to be mainly due to the significant curvature of the filaments corresponding to a non-uniform strain and strain rate throughout the filament. The determination of an elongational viscosity would require a full three dimensional simulation of the whole experiment using appropriate constitutive equations and an additional measurement of the force acting on the end plates. But this is beyond the scope of this paper. Therefore, we discuss the determination of appropriate parameters describing extensional flow

Figure 6 (left): The transient diameter at the neck measured for the w/o emulsion using linear velocity stretching profile $v = 0.34$ mm/s and plate separation distances $h_o = 3$ mm and $h_i = 16.64$ mm. The dashed and solid lines show the predictions for the power law and the Bingham models, respectively.

Figure 7: Typical light intensity profile perpendicular to the filament axis.

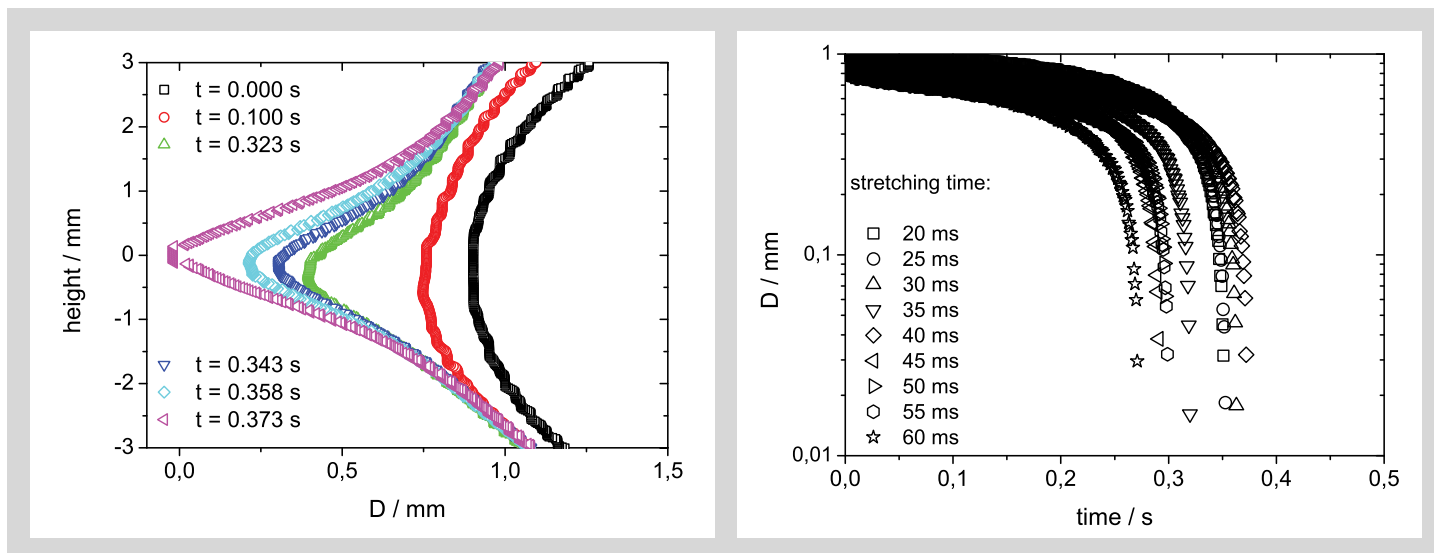


Figure 8 (left): Typical results for time evolution of filament profile.

Figure 9: Influence of stretching time on the time evolution of the diameter at the neck. The experiments were performed for w/o emulsion using linear velocity stretching profile and plate separation distances $h_o = 3 \text{ mm}$ and $h_f = 16.64 \text{ mm}$.

behavior of fluids with yield stress in CaBER experiment. For quantitative comparison of non-cylindrical filaments, description of full filament shape is needed.

For this issue an image analysis software has been developed. The filament edges are detected based on a scan of light intensity perpendicular to the filament axis (see Figure 7). Pixels of high and low light intensities represent the bright background field and dark filament profile, respectively. The edges of the filament are identified, when the light intensity drop below given threshold limit, which is chosen with respect to background intensity and noise level. Due to telecentric optics and illumination filament edges are well defined and can be determined with an accuracy of ± 1 pixel. The filament diameter is calculated as a difference between the two edges.

A typical result for the time evolution of the filament shape is shown in Figure 8. It is noticeable that in the lower and in the upper parts of the filament, the diameter hardly changes. The thinning process takes place in a very restricted volume. Therefore, it seems to be reasonable to characterize the thinning process by the region within thinning takes place and the time evolution of the filament curvature at the neck, in addition to the transient neck diameter. This region of deformation is characterized here by the distance l_{def} between the upper and lower position along the filament axis where no change in diameter is detected. In cylindrical coordinates, the curvature is given by:

$$\kappa = \left| \frac{\left(\frac{\partial^2 R_1}{\partial h^2} \right)}{\left[1 + \left(\frac{\partial R_1}{\partial h} \right)^2 \right]^{3/2}} \right| \quad (3)$$

where h is the filament height and R_1 is the filament radius. There is no analytical function to

describe the diameter as a function of vertical position, thus it is more convenient to calculate the derivatives numerically, directly from the experimental data. In order to get reliable results it is recommended to smooth the data before differentiating. Here, we have used a conventional cubic smoothing spline method [32].

3 RESULTS AND DISCUSSION

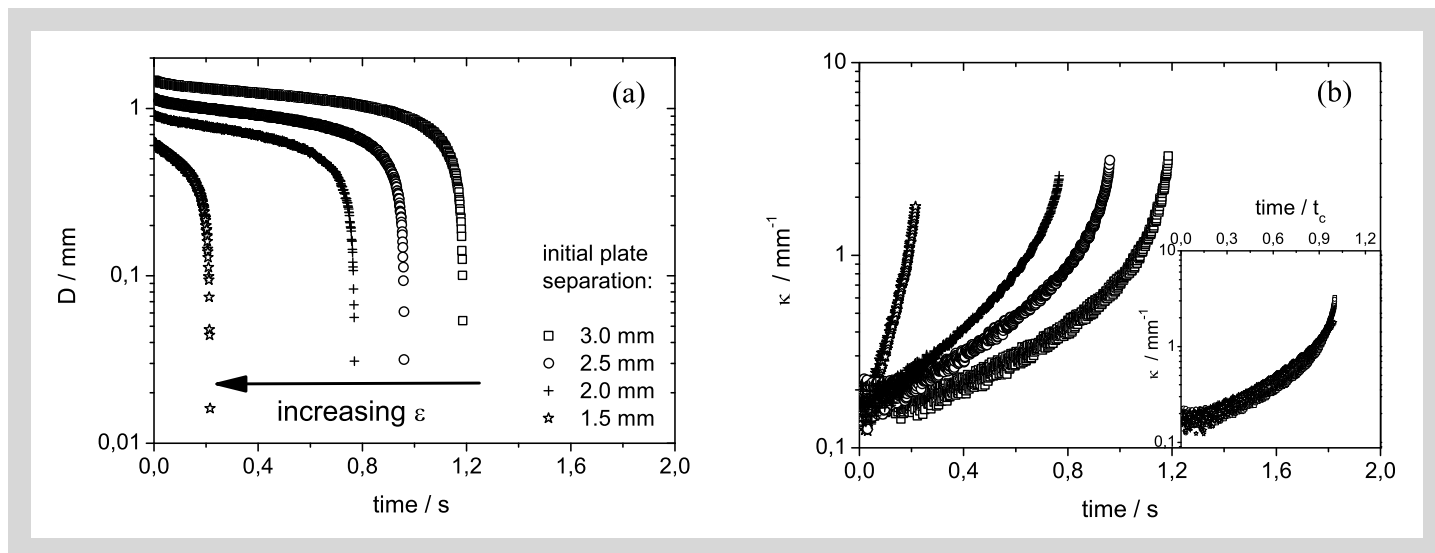
In the following the influence of the initial setting parameters of CaBER experiments is discussed. We have varied:

- stretching time t_s
- stretching velocity profile
- final plate separation h_f at constant h_o (and vice versa). This corresponds to a variation of Hencky strain
- initial and final plate separation h_o and h_f , respectively in such a way that ϵ is kept constant, but the sample volume varies proportional to h_o .

The capillary number, $Ca = \eta_s \dot{\epsilon} d / 2\sigma$ in the initial step strain of the CaBER experiment is in order of 10^{-5} for the emulsion investigated here. Therefore, we do not expect droplet deformation or breakup to be relevant in this part of the CaBER experiment.

3.1 INFLUENCE OF STRETCHING TIME

The influence of stretching time on the elongation properties of the yield stress fluids was tested for stretching times between 20 ms (lower device limit) and 60 ms, in steps of $\Delta t = 5 \text{ ms}$. The experiments were performed using linear stretching profile. The plate distances were set to: initial gap $h_o = 3.00 \text{ mm}$, final gap $h_f = 16.64 \text{ mm}$. For each stretching time we have performed at least five measurements. The resulting representative curves for the time evolution of the filament diameter at the neck corresponding to each t_s are shown in Figure 9. Though the dis-



crepancies between these results are remarkable, there is no systematic variation of filament life time, t_c and region of deformation with stretching time. The mean values and corresponding standard deviation calculated from the results of the repeated measurements are $t_c = 0.321 \text{ s} \pm 12 \%$ and $l_{def} = 2.118 \text{ mm} \pm 6 \%$. To select the most appropriate stretching time for the experiments one has to compromise. If the plate separation is too rapid the fluid filament is unstable and flatters. On the other hand, step strain experiments require ideally infinitesimal short deformation time. Thus, most appropriate values are between 35 ms and to 50 ms.

3.2 INFLUENCE OF STRETCHING PROFILE

There are three stretching profiles available in the commercial firmware for the CaBER 1 provided by Thermo Haake. Linear, where the plates are separated with constant velocity. Exponential, here the velocity of the plate increase exponentially. Lastly cushioned profile, here at the beginning the plates are separated with constant velocity corresponding to the fastest stretching time, but in order to reduce problems caused by the rapid deceleration, at the end plate motion slows down exponentially.

Measurements for each stretching profile were performed with the stretching time 40 ms. The plates distances were again set $h_o = 3.00 \text{ mm}$ and $h_f = 16.64 \text{ mm}$. For the cushioned profile the neck is slightly higher compared to the two other profiles. Nevertheless, the time evolution of the filament diameter at the neck is nearly identical in all cases. Mean values and standard deviations of filament life time and deformation volume as obtained from at least 5 repeated measurements under the same experimental conditions are shown in Table 1. Obviously, the cushioned profile yields the highest accuracy for these parameters.

	linear	exponential	cushioned
t_c	$0.36 \text{ s} \pm 6 \%$	$0.34 \text{ s} \pm 3 \%$	$0.35 \text{ s} \pm 3 \%$
l_{def}	$1.97 \text{ mm} \pm 5 \%$	$2.23 \text{ mm} \pm 7 \%$	$2.16 \text{ mm} \pm 4 \%$

3.3 INFLUENCE OF PLATE SEPARATION

In this section influence of the geometrical stretching parameters on filament thinning of the yield stress fluids is discussed. A first set of experiments was performed with different initial heights $h_{o1} = 1.50 \text{ mm}$, $h_{o2} = 2.00 \text{ mm}$, $h_{o3} = 2.50 \text{ mm}$, $h_{o4} = 3.00 \text{ mm}$. The plates were always moved to the same end distance, $h_f = 11.17 \text{ mm}$. Accordingly, increase of h_o leads to a decrease of the Hencky strain during filament formation. Stretching time was constant for all measurements and equal to 40 ms. For good statistics, the measurements were repeated several times. The representative results for the time evolution of filament diameter at the neck is shown in Figure 10a. As expected with increasing initial gap, i.e. increasing sample volume the initial filament diameter is larger and filament life time is longer. Moreover, it seems that the filament shape is not influenced by the Hencky strain. The curvature measured at the neck shows similar time evolution starting always with the same initial value (Figure 10b).

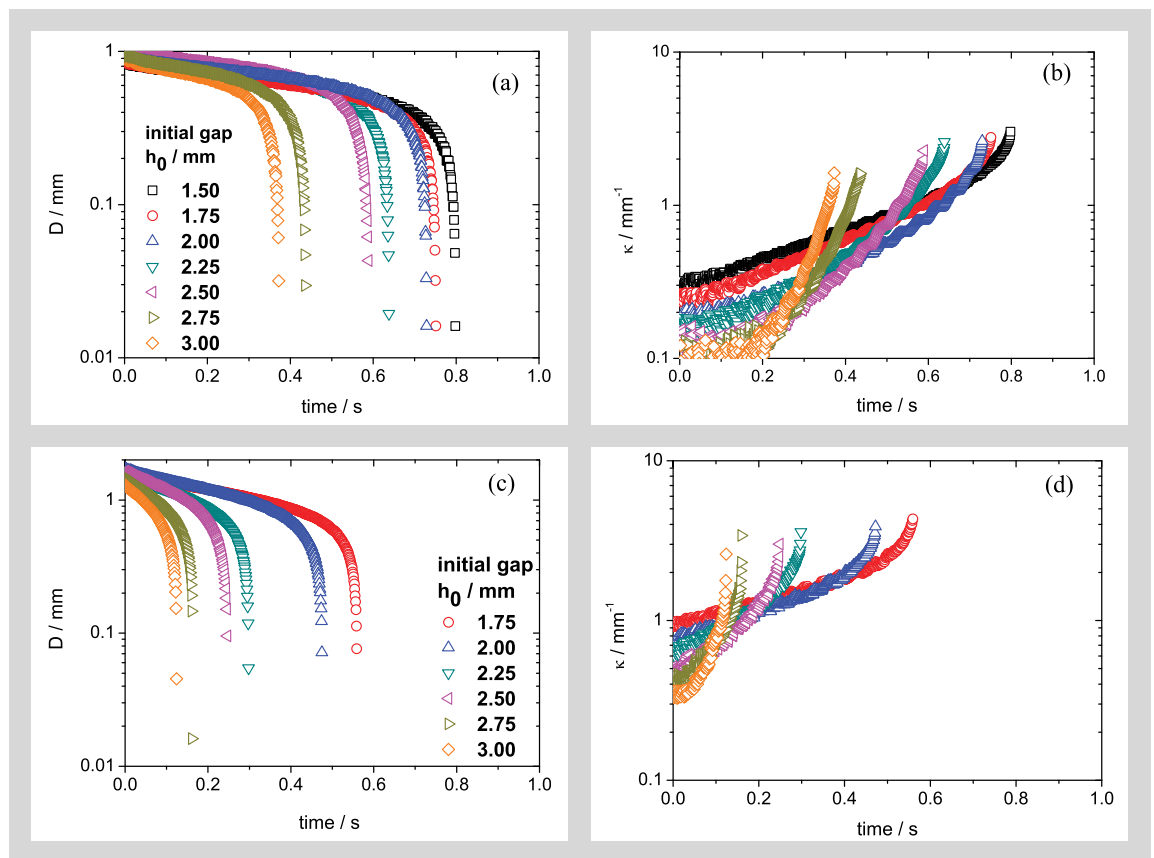
Similar effects are observed while varying the end distance, h_f and keeping the initial gap constant. Here, the constant sample volume is stretched more when h_f is increased. Thus, the filament diameter is smaller and filament life time is shorter for larger h_f .

Finally, the initial and the end distances were varied in order to keep the Hencky strain constant. The measurements were performed for the initial gap in the range between $h_o = 1.50 \text{ mm}$ and $h_o = 3.00 \text{ mm}$ in steps of $\Delta h_o = 0.25 \text{ mm}$ (in the case of the thickener solution the smallest initial gap was $h_o = 1.75 \text{ mm}$). The end distance was adjusted in the way that the Hencky strain

Figure 10: Influence of imposed Hencky strain, ϵ on time evolution of diameter (a) and curvature (b) at the neck. Experiments were performed for w/o emulsion using linear velocity stretching profile and stretching time $t_s = 40 \text{ ms}$, ϵ was changed by changing h_o , while the end distance $h_f = 11.17 \text{ mm}$ was kept constant. The inset in lower right corner of figure (b) shows results rescaled with respect to the filament life time, t_c .

Table 1: Experimental results for filament life time and deformation volume measured with different velocity stretching profiles.

Figure 11: Influence of plate separation distances, h_o and h_f at constant Hencky strain $\epsilon = 1.71$ for the w/o emulsion (a) and (b) and $\epsilon = 1.21$ for the thickener solution (c) and (d). Figures (a) and (c) show time evolution of the diameter at the neck and figures (b) and (d) show accordingly time evolution of the curvature.



was always equal to $\epsilon = 1.71$ for the w/o emulsion and $\epsilon = 1.21$ for the thickener solution. The measurements were performed using linear stretching profile and stretching time $t_s = 40$ ms. As before the measurements were repeated several times. Representative curves for the time evolution of diameter and curvature at the neck are shown in Figure 11. It can be seen that, although the plate distance is varied, the initial value of the diameter at the neck D_o does not change when Hencky strain is constant. But the filament life time is systematically shorter for larger separations. At the same time the curvature at the thinning point decreases with increasing plate separation.

The filament thinning process is determined by the balance between visco-elastic and capillary forces. The visco-elastic forces are material specific, i.e. they are equal in each experiment. The capillary forces are determined by the Laplace pressure, which for curved filament shape is given by:

$$\Delta p = \sigma \left(\frac{1}{R_1} + \frac{1}{R_2} \right) \quad (4)$$

here R_1 is the filament radius and $R_2 = 1/\kappa$ is the radius of curvature. For concave shape of the filament, R_2 is always negative. If plate distance is changed in a way that keeps Hencky strain constant the initial filament diameter does not change, but the initial curvature increases with

decreasing h_o (Figure 11). This corresponds to a reduced Laplace pressure and hence filament life time is longer. The contribution of the filament curvature, $1/R_2$ to the Laplace pressure is shown in Figure 12.

On the other hand, when Hencky strain is changed by varying either h_o or h_f the initial diameter increases with decreasing ϵ while the initial curvature is essentially constant (Figure 10). Here Laplace pressure changes are due to the first term in Eq. 4 and Δp increases with increasing ϵ and accordingly, filament life time decreases.

4 CONCLUSION

Application range of the capillary breakup extensional rheometer for investigations of extensional flow properties of high viscosity yield stress fluids was tested. A w/o emulsion and a polymeric thickener solution were used as model systems. Both samples are characterized by similar apparent yield stress ($\tau_y \approx 10$ Pa) but they have distinctly different low shear viscosities. Both yield stress fluids exhibit inhomogeneous filament thinning with a strongly concave filament shape. The shape of the $D(t)$ -curves is also very similar. However, the thickener solution with the lower steady shear viscosity has accordingly shorter filament life time. Analysis of full filament shapes requires an advanced set-up for image acquisition and processing. This includes a high speed camera, telecentric objective and illumination, as well as an image analysis soft-

ware. The time evolution of the full filament contour is detected with resolution of ± 1 pixel.

The influence of the stretching parameters of the CaBER device on capillary thinning of fluids with an apparent yield stress was discussed. Neither stretching time nor stretching velocity profile has significant influence on the capillary thinning of those fluids. Suggested initial set-up parameters are cushioned stretching profile, which provides the best reproducible results and optimal stretching time is in the range between 35 ms and 50 ms. Variation of Hencky strain, results in a decrease of initial diameter and filament life time with increasing ϵ , but it has no influence on the initial curvature. Moreover, diameter and curvature at the neck, measured for different ϵ show similar time evolution. Lastly, if plate separation is varied in a way that keeps Hencky strain unchanged, the initial value of diameter remains constant but the curvature increases with decreasing initial gap separation and results in a deceleration of the thinning process according to the corresponding drop of the Laplace pressure inside the filament.

Although further efforts are required for a determination of physical quantities like elongational viscosity, the CaBER technique can be successfully applied to investigate elongational flow properties of yield stress fluids. The time- and space- evolution of the fluid filament can be quantified. The measurement technique gives well reproducible results, variation in the characteristic parameters extracted from the filament profiles do not exceed 10 %. Thus, future work will address influence of fluid properties, e.g. volume fraction of disperse phase and droplet size for the emulsions or polymer concentration and pH value for the thickener solutions, on capillary thinning. The determination of an elongational yield stress and the identification of rheological parameters characterizing the transient extensional properties of such fluids which can be correlated to processing and application properties will be of particular interest.

ACKNOWLEDGMENT

We would like to thank Prof. Dr. Stephan Naser (Hochschule Darmstadt, Germany) for interesting discussions and advice regarding the optical set-up and image analysis. We greatly acknowledge donation of Sterocoll®D by BASF SE and we

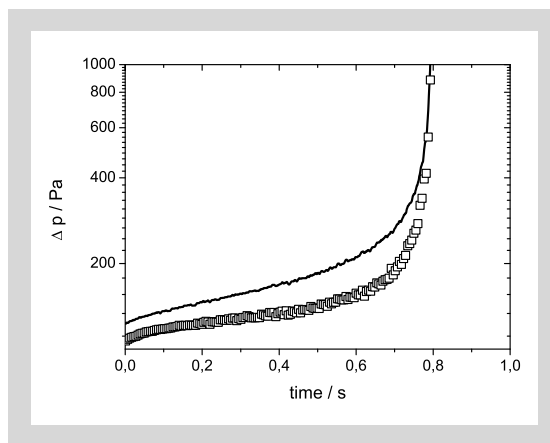


Figure 12: Influence of filament curvature on Laplace pressure. The open symbols show the Laplace pressure calculated from Eq. 4 using the data from Figure 11 (a) and (b). The initial plate distance was $h_0 = 1.5$ mm, and end plate distance, $h_f = 16.64$ mm. Solid line was calculated neglecting the filament curvature, i.e. $R_2 = 0$.

thank Anne Kowalczyk for her help in preparation of Sterocoll®D solution and performing CaBER experiments on it. Further we thank Kompetenznetz Verfahrenstechnik Pro3 e.V. and Beiersdorf AG for the financial support.

REFERENCES

- [1] Plateau J: Experimental and theoretical researches on the figures of equilibrium of a liquid mass withdrawn from the action of gravity, Annu. Rep. Smithsonian Inst. (1863) 207–285.
- [2] Lord Rayleigh: On the stability of jets, Proc. London Math. Soc. 10 (1879) 4–13.
- [3] Sridhar T, Tirtaatmadja V, et al.: Measurement of extensional viscosity of polymer solutions, J. Non-Newtonian Fluid Mech. 40 (1991) 271–280.
- [4] Tirtaatmadja V, Sridhar T: A filament stretching device for measurement of extensional viscosity, J. Rheol. 37 (1993) 1081–1102.
- [5] Entov VM, Hinch EJ: Effect of a spectrum of relaxation times on the capillary thinning of a filament of elastic liquid, J. Non-Newtonian Fluid Mech. 72 (1997) 1081–1102.
- [6] Rodd LE, Scott TP, et al.: Capillary break-up rheometry of low-viscosity elastic fluids, Appl. Rheol. 15 (2004) 12–27.
- [7] Basilevskii AV, Entov VM, et al.: Failure of Polymer Solution Filaments, Polym. Sci. A 39 (1997) 316–324.
- [8] Basilevskii AV, Entov VM, et al.: Failure of an Oldroyd Liquid Bridge as a Method for Testing the Rheological Properties of Polymer Solutions, Polym. Sci. A 43 (2001) 1161–1172.
- [9] Clasen C, Plog JP, et al.: How dilute are dilute solutions in extensional flows?, J. Rheol. 50 (2006) 849–881.
- [10] Solomon MJ, Muller SJ: The transient extensional behavior of polystyrene-based Boger fluids of varying solvent quality and molecular weight, J. Rheol. 40 (1996) 837–856.
- [11] Rothstein JP: Strong flows of viscoelastic wormlike micelle solutions, Rheol. Rev. (2008) 1–42.
- [12] Bhardwaj A, Miller E, et al.: Filament stretching and capillary breakup extensional rheometry measurements of viscoelastic wormlike micelle solutions, J. Rheol. 51 (2007) 693–719.
- [13] McKinley GH: Visco-elasto-capillary thinning and break-up of complex fluids, Rheol. Rev. (2005) 1–48.
- [14] Kheirandish S, Guybaidullin I, et al.: Shear and elongational flow behavior of acrylic thickener

- solutions, Part I: Effect of intermolecular aggregation, *Rheol. Acta* 47 (2008) 999–1013.
- [15] Kheirandish S, Guybaidullin I, et al.: Shear and elongational flow behavior of acrylic thickener solutions, Part II: effect of gel content, *Rheol. Acta* 48 (2009) 397–407.
- [16] Renardy M, Renardy Y: Similarity solution for breakup of jets of power law fluids, *J. Non-Newtonian Fluid Mech.* 122 (2004) 303–312.
- [17] Renardy M: Similarity solution for jet breakup for various models of viscoelastic fluids, *J. Non-Newtonian Fluid Mech.* 104 (2002) 65–74.
- [18] Renardy M: Self-similar breakup of Giesekus jet, *J. Non-Newtonian Fluid Mech.* 97 (2001) 261–293.
- [19] Renardy M: Self-similar jet breakup for generalized PPT model, *J. Non-Newtonian Fluid Mech.* 103 (2002) 261–269.
- [20] Yildirim OE, Basaran OA: Deformation and breakup of stretching bridges of Newtonian and shear-thinning liquids: comparison of one- and two-dimensional models, *Chem. Eng. Sci.* 56 (2001) 211–233.
- [21] Ambravaneswaran B, Basaran OA: Effect of insoluble surfactants on the nonlinear deformation and breakup of stretching liquid bridges, *Phys. Fluids* 11 (1999) 997–1015.
- [22] Webster MF, Matallah H, et al.: Numerical modeling of step-strain for stretched filaments, *J. Non-Newtonian Fluid Mech.* 151 (2008) 38–58.
- [23] Oliveira MSN, Yeh R, et al.: Extensional Rheology and Formation of Beads-on-a-String Structures in Polymer Solutions, *J. Non-Newtonian Fluid Mech.* 137 (2006) 137–148.
- [24] Stelter M, Brenn G, et al.: Validation and application of a novel elongational device for polymer solutions *J. Rheol.* 44 (2000) 595–616.
- [25] McKinley GH, Tripathi A: How to extract the Newtonian viscosity from capillary breakup measurements in a filament rheometer, *J. Rheol.* 44 (2000) 653–670.
- [26] Lowry BJ, Steen PH: Capillary Surfaces: Stability from Families of Equilibria with Application to the Liquid Bridge, *Proc. R. Soc. London, A* 449 (1995) 411–439.
- [27] Mahajan MP, Tsige M, et al.: Stability of liquid crystalline bridges, *Phys. Fluids* 11 (1999) 491–493.
- [28] Goldin M, Pfeffer R, et al.: Break-up of a capillary jet of a non-Newtonian fluid having a yield stress, *Chem. Eng. J.* 4 (1972) 8–20.
- [29] Rothstein JP, Miller E, et al.: The Effect of Step-Stretch Parameters on Capillary Breakup Extensional Rheology (CaBER) Measurements, *Proc. Int. Cong. Rheol.* (2008).
- [30] Sattler R, Wagner C, et al.: Blistering Pattern and Formation of Nanofibers in Capillary Thinning of Polymer Solutions, *Phys. Rev. Lett.* 100 (2008) 164502.
- [31] Smith WJ: *Modern optical engineering*, 3rd Edition, McGraw-Hill, New York (2000).
- [32] Bowman AW, Azzalini A: *Applied Smoothing Techniques for Data Analysis: the Kernel Approach with S-Plus Illustrations*, Oxford University Press (1997).

